J Fluoresc (2014) 24:1169–1176
DOI 10.1007/s10895-014-1397-9

ORIGINAL PAPER

Molecular Keypad Locks Based on Gated Photochromism and Enhanced Fluorescence by Protonation Effects

Ming-Hua Zheng · Wei Sun · Jing-Yi Jin · Chun-Hua Yan

Received: 11 February 2014 / Accepted: 7 April 2014 / Published online: 22 April 2014

Abstract Being a "lock-unlock" system, gated photochromism is generally applied in nondestructive readout for optical memory materials. In the presented paper, we successfully constructed molecular keypad locks by introduction of the gated photochromism. A series of diarylethenes compounds (DAEs) based on fluorescent 5-methoxy-2-pyridyl thiazoles, were prepared and then characterized as photochromic fluorescent switches. Protoantion of the reported DAEs resulted in both protonation-locked photo-reactivities, i.e., gated photochromism, and enhancement of fluorescence. Molecular keypad locks were then successfully constructed, which are also featured by "one-key" lock operation.

Keywords Diarylethenes · Photochromism · Fluorescence · Protonation · Logic function · Molecular keypad lock

Introduction

Photochromism is defined as a reversible photo-induced transformation of a molecule between two isomers with different absorption spectra accompanied by other photo-switching effects, such as changes in fluorescent intensities, magnetic properties, geometrical structures, and so on [1]. Being the analog of Boolean algebra, photochromic fluorescence switches have been widely applied in various technologies, such as data storage and digital information processing at the molecular level [2–7]. For example, a fluorescent diarylethene (DAE) compound was reported as a good candidate for non-destructive readout of ultrahigh-density single molecule optical memory [8]. The other concept related to the non-destructive readout is gated photochromism [9–14], which is featured by the controlled photochromic properties. As shown in Chart 1a, the "locked" form is inert for the other external optical excitation and then regarded as an appreciated state for a non-destructive readout in optical data storages [9]. Further, it can be found that transformation from **O-H**$^+$ to **C-H**$^+$ should follow the input string sequences as "base→UV→acid" as exemplified in the ref. 4b (Chart 1a). Such request in the input sequence is similar to the one in the case of molecular keypad lock; which play the essential roles in the protection of digital information by authorizing password entries at the molecular scale [15, 16]. Up to now, some fluorescent DAEs have been developed as molecular keypad locks [17–20], where the design rationale to construct the "lock-unlock" system were based on the unsymmetrical DAEs with fluorescent sensing. As shown in Chart 1b, we hope to report a new approach to molecular keypad lock based on the conscription of gated photochromism as well as the enhanced fluorescence caused by protonation effects.

The presented DAE compounds are derivatives of 5-methoxy-2-pyridyl thiazoles (**MPT**s) reported previously [21]. Here we successfully prepared five **MPT**-based DAEs as shown in Scheme 1. For three symmetrical DAEs, both **1a** and **1d** could be synthesized by either one or two steps. However, the other symmetrical DAE could not be obtained, which should be ascribed to the unexpected arrangement of the deprotonated **4-MPT** [22]. Other three unsymmetrical **MPT**-based DAEs (**1b–c**, **1e**) could be smoothly obtained from the 2- or 3-**MMPT**. Protonation of the DAE systems

Electronic supplementary material The online version of this article (doi:10.1007/s10895-014-1397-9) contains supplementary material, which is available to authorized users.

M.-H. Zheng · J.-Y. Jin (✉)
Department of Chemistry, Yanbian University, Yanji City, Jilin Province 133002, China
e-mail: jyjin-chem@ybu.edu.cn

M.-H. Zheng · W. Sun · C.-H. Yan
Beijing National Laboratory for Molecular Sciences, State Key Lab of Rare Earth Materials Chemistry and Applications & PKU-HKU Joint Lab in Rare Earth Materials and Bioinorganic Chemistry, Peking University, Beijing 100871, China

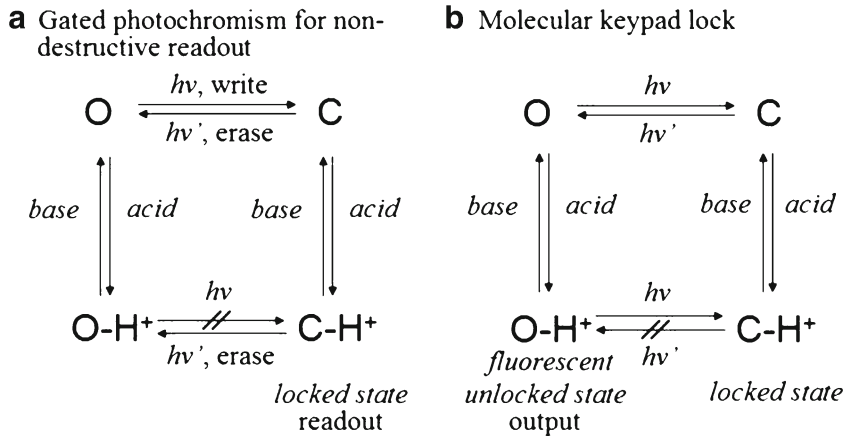

Chart 1 **a** Gated photochromism for nondestructive readout. **b** Molecular keypad lock

could provide gated photochromism as well as enhancement of fluorescence. We then propose an alternative approach to molecular keypad locks based on gated photochromism (Scheme 2).

Experimental

Material and Methods

All reactions were performed under argon atmosphere using the purified solvents by standard methods. All chemicals were purchased from Acros, and used as received without further purification. For all spectrometric measurement, HPLC grade solvents were not degassed and used as received. For chromatography, 100–200 mesh silica gel (Qingdao, China) was employed.

UV–vis absorption spectra were measured with an absorption spectrophotometer (Hitachi U-3010) and fluorescence spectra were determined on a fluorescence spectrophotometer (Hitachi F-4500). NMR spectra were recorded at a Varian Mercury 200 or 300 spectrometer. Chemical shifts are reported in ppm using tetramethylsilane (TMS) as the internal standard. IR spectra were recorded with a Nicolet 5MX-S infrared spectrometer. Mass spectra were obtained on a VG ZAB-HS mass spectrometer and a Finnigan LCQ mass spectrometer. Elemental analyses were performed at Peking University, Beijing, China.

All spectra measurements were taken at 20 °C. Unless mentioned otherwise, photochromic behaviors were determined at the concentration of 2.5×10^{-5} M in dichloromethane. Photo-irradiation was carried out by using 150 W Xeon arc lamp as the exciting light source equipped on Hitachi F-4500 fluorescence spectrophotometer. Irradiation wavelengths were selected by passing the light through a monochrometer (5 nm slit) on Hitachi F-4500 fluorescence spectrophotometer.

Synthesis

General Procedures to 4-bromo-5-methoxy-2-pyridyl Thiazoles (BMPTs)

The corresponding **MPT** (390 mg, 2.03 mmol) was dissolved in 10 mL dried chloroform. *N*-Bromosuccimide (433 mg, 2.43 mmol) was added and then allowed to be stirred overnight under Ar atmosphere. The reaction was quenched by addition of sodium bicarbonate aqueous solution and then extracted with ethyl acetate (15 mL×3). The organic layer was dried over Na_2SO_4, followed by evaporation under reduced pressure. The obtained oil was purified by silica gel chromatography using *n*-hexane and ethyl acetate as eluent. 4-Bromo-5-methoxy-2-pyridyl thiazole was isolated as white solid.

4-Bromo-5-methoxy-2-(2-pyridyl) thiazole (**2-BMPT**)

Yield, 93.6 %. M.p.: 115–116 °C (Dec.). IR (KBr, cm^{-1}): 1,538, 1,529, 1,487, 1,435, 1,420, 1,296, 1,247, 1,004, 849, 784. ^{1}H NMR ($CDCl_3$, 200 MHz): δ=8.54–8.52 (m, 1H), 8.10–8.06 (m, 1H), 7.79–7.73 (m, 1H), 7.31–7.25 (m, 1H), 4.07 (s, 3H). ^{13}C NMR ($CDCl_3$, 50 MHz): δ=158.0, 150.6, 149.2, 137.0, 124.3, 118.6, 116.0, 108.3, 63.6. Calcd. for $C_9H_7N_2OSBr$: 269.9462, HRMS m/z: 269.9459. Anal. Calcd for $C_9H_7N_2OSBr$: C 39.87, H 2.60, N 10.33; Found: C 39.97, H 2.59, N 10.41.

4-Bromo-5-methoxy-2-(3-pyridyl) thiazole (**3-BMPT**)

Yield, 94.5 %. M.p.: 110–111 °C. IR (KBr, cm^{-1}): 1,536, 1,485, 1,462, 1,424, 1,329, 1,279, 1,250, 994, 850, 700. ^{1}H NMR ($CDCl_3$, 200 MHz): δ=9.01–9.00 (m, 1H), 8.64–8.62 (m, 1H), 8.17–8.11 (m, 1H), 7.39–7.33 (m, 1H), 4.06 (s, 3H). ^{13}C NMR ($CDCl_3$, 50 MHz): δ=151.6, 150.6, 146.5, 132.5, 129.3, 123.7, 116.0, 109.3, 64.0. Calcd. for $C_9H_7N_2OSBr$: 269.9462, HRMS m/z: 269.9463. Anal. Calcd for $C_9H_7N_2OSBr$: C 39.87, H 2.60, N 10.33; Found: C 39.88, H 2.64, N 10.23.

Scheme 1 Synthesis of the **MPT**-based DAEs

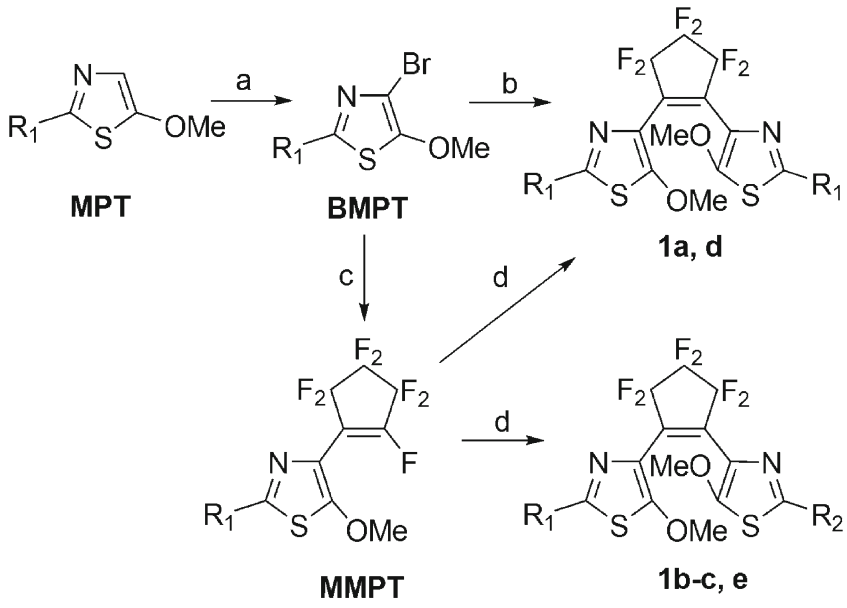

R_1 = 2-py: 2-**MPT**, 2-**BMPT**, 2-**MMPT**, **1a**;
3-py: 3-**MPT**; 3-**BMPT**, 3-**MMPT**, **1d**;
4-py: 4-**MPT**; 4-**BMPT**;
R_1 = 2-py, R_2 = 3-py: **1b**;
R_2 = 4-py: **1c**;
R_1 = 3-py, R_2 = 4-py: **1e**.

a. NBS; b. *n*-BuLi, 0.5 eq. PFCP, -78 °C;
c. *n*-BuLi, 1.0 eq PFCP, -78 °C; d. *n*-BuLi, 1.0 eq. **BMPT**, -78 °C.

Scheme 2 Schematic representation of the gated-photochromism and molecular keypad lock in the presented paper

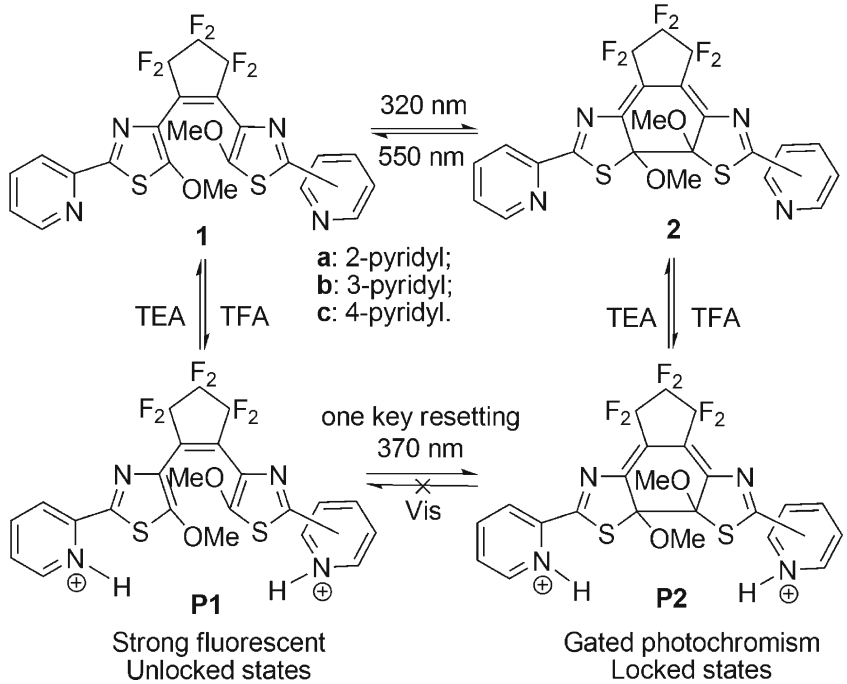

4-Bromo-5-methoxy-2-(4-pyridyl) thiazole (**4-BMPT**)

Yield, 96.1 %. M.p.: 113–114 °C (Dec.). IR (KBr, cm^{-1}): 1,594, 1,533, 1,497, 1,432, 1,409, 1,324, 1,287, 1,254, 1,175, 1,005, 855, 813. ^{1}H NMR ($CDCl_3$, 200 MHz): δ=8.67 (d, J=4.5 Hz, 2H), 7.68 (d, J=4.5 Hz, 2H), 4.08 (s, 3H). ^{13}C NMR ($CDCl_3$, 50 MHz): δ=156.7, 151.4, 150.6, 139.9, 118.9, 109.6, 64.1. Calcd. for $C_9H_7N_2OSBr$: 269.9462, HRMS m/z: 269.9458. Anal. Calcd for $C_9H_7N_2OSBr$: C 39.87, H 2.60, N 10.33; Found: C 39.88, H 2.41, N 10.32.

*General Procedures to 1-[(5-methoxy-2-pyridyl)thiazin-4-yl] perfluorocyclopentenes (***MMPT***s)*

To a stirring solution of **BMPT** (530 mg, 1.95 mmol) in dried THF (25 mL) was slowly added 2.87 M *n*-BuLi in *n*-hexane (0.75 mL, 2.1 mmol) at −78 °C under Ar atmosphere. After the mixture had been stirred for 30 min at −78 °C, perfluorocyclopentene (428 mg, 1.95 mmol) in dried THF (5 mL) was added. The reaction mixture was further stirred at −78 °C for 3 h, and then 1 M hydrochloride was added. The product was extracted with ethyl acetate, dried with Na_2SO_4, and concentrated under reduced pressure. The residue was purified by silica gel chromatography using *n*-hexane and ethyl acetate as eluent to afford the needed compound.

1-[5-methoxy-2-(2-pyridyl)thiazin-4-yl] perfluorocyclopentene (**2-MMPT**)

Yield, 53.8 %. M.p.: 119–120 °C. IR (KBr, cm^{-1}): 1,695, 1,585, 1,525, 1,510, 1,436, 1,392, 1,345, 1,332, 1,296, 1,282, 1,193, 1,144, 1,117, 994, 977, 949, 786. ^{1}H NMR ($CDCl_3$, 300 MHz): δ=8.57–8.55 (m, 1H), 8.15–8.11 (m, 1H), 7.84–7.76 (m, 1H), 7.35–7.29 (m, 1H), 4.15 (s, 3H). ^{13}C NMR ($CDCl_3$, 75 MHz): δ=167.6, 155.8, 150.7, 149.2, 137.1, 124.6, 120.9, 119.0, 116.4, 110.9, 64.4. Calcd. for $C_{14}H_7N_2OSF_7$: 384.0167, HRMS m/z: 384.0170. Anal. Calcd for $C_{14}H_7N_2OSF_7$: C 43.76, H 1.84, N 7.29; Found: C 43.68, H 1.70, N 7.17.

1-[5-methoxy-2-(3-pyridyl)thiazin-4-yl] perfluorocyclopentene (**3-MMPT**)

Yield, 33.2 %. M.p.: 90.5–92 °C. IR (KBr, cm^{-1}): 1,679, 1,526, 1,510, 1,404, 1,348, 1,330, 1,284, 1,194, 1,139, 1,112, 1,075, 991, 978, 941, 810, 750. ^{1}H NMR ($CDCl_3$, 300 MHz): δ=9.02–9.01 (m, 1H), 8.65–8.64 (m, 1H), 8.20–8.16 (m, 1H), 7.41–7.37 (m, 1H), 4.15 (s, 3H). ^{13}C NMR ($CDCl_3$, 75 MHz): δ= 165.5, 155.7, 151.3, 150.9, 146.9, 132.9, 129.2, 123.8, 115.8, 110.8, 64.8. Calcd. for $C_{14}H_7N_2OSF_7$: 384.0167, HRMS m/z: 384.0168. Anal. Calcd for $C_{14}H_7N_2OSF_7$: C 43.76, H 1.84, N 7.29; Found: C 43.80, H 1.84, N 7.26.

General Procedures to the MPT-based DAEs from **MMPT***s*

To a stirring solution of **BMPT** (272 mg, 1.0 mmol) in dried THF (10 mL) was slowly added 2.87 M *n*-BuLi in *n*-hexane (0.42 mL, 1.2 mmol) at −78 °C under argon atmosphere. After the mixture had been stirred for 30 min at −78 °C, **MMPT** (256 mg, 0.67 mmol) in dried THF (5 mL) was added. The reaction mixture was further stirred at −78 °C for 3 h, and then 1 M hydrochloride was added. The product was extracted with ethyl acetate, dried with Na_2SO_4, and concentrated under reduced pressure. The residue was purified by silica gel chromatography using n-hexane and ethyl acetate as eluent to afford the products.

1,2-bis[5-methoxy-2-(2-pyridyl)thiazin-4-yl] perfluorocyclopentene (**1a**)

Yield, 35.6 %. ^{1}H NMR ($CDCl_3$, 300 MHz): δ=8.55–8.53 (m, 2H), 8.08–8.05 (m, 2H), 7.78–7.73 (m, 2H), 7.31–7.27 (m, 2H), 3.85 (s, 6H). ^{13}C NMR ($CDCl_3$, 75 MHz): δ=154.2, 151.0, 149.1, 137.1, 124.3, 119.0, 117.7, 101.2, 64.0. Calcd. for $C_{23}H_{14}N_4O_2S_2F_6$: 556.0462, HRMS m/z: 556.0467. Anal. Calcd for $C_{23}H_{14}N_4O_2S_2F_6$: C 49.64, H 2.54, N 10.07; Found: C 49.50, H 2.30, N 10.05.

1-[5-methoxy-2-(2-pyridyl)thiazin-4-yl]-2-[5-methoxy-2-(3-pyridyl)thiazin-4-yl]perfluorocyclopentene (**1b**)

Yield, 30.1 %. ^{1}H NMR ($CDCl_3$, 300 MHz): δ=8.99–8.98 (m, 1H), 8.62–8.61 (m, 1H), 8.54–8.53 (m, 1H), 8.17–8.14 (m, 1H), 8.04–8.01 (m, 1H), 7.77–7.72 (m, 1H), 7.38–7.34 (m, 1H), 7.31–7.27 (m, 1H), 3.87 (s, 3H), 3.86 (s, 6H). ^{13}C NMR ($CDCl_3$, 75 MHz): δ=165.9, 163.5, 154.4, 150.9, 150.5, 149.7, 149.1, 146.7, 137.0, 132.8, 129.5, 126.5, 126.2, 124.3, 123.8, 119.0, 118.9, 116.0, 64.4, 64.0. Calcd. for $C_{23}H_{14}N_4O_2S_2F_6$: 556.0462, HRMS m/z: 556.0468. Anal. Calcd for $C_{23}H_{14}N_4O_2S_2F_6$: C 49.64, H 2.54, N 10.07; Found: C 49.80, H 2.56, N 9.66.

1-[5-methoxy-2-(2-pyridyl)thiazin-4-yl]-2-[5-methoxy-2-(4-pyridyl)thiazin-4-yl]perfluorocyclopentene (**1c**)

Yield, 10.9 %. ^{1}H NMR ($CDCl_3$, 300 MHz): δ=8.66–8.64 (m, 2H), 8.55–8.53 (m, 1H), 8.02–7.99 (m, 1H), 7.77–7.72 (m, 1H), 7.68–7.66 (m, 2H), 7.32–7.27 (m, 1H), 3.87 (s, 3H), 3.86 (s, 6H). ^{13}C NMR ($CDCl_3$, 75 MHz): δ=166.0, 164.3, 154.4, 150.8, 150.5, 150.4, 149.8, 149.1, 140.2, 137.0, 126.8, 126.0, 124.3, 121.1, 119.3, 118.8, 64.4, 64.0. Calcd. for $C_{23}H_{14}N_4O_2S_2F_6$: 556.0462, HRMS m/z: 556.04667. Anal. Calcd for $C_{23}H_{14}N_4O_2S_2F_6$: C 49.64, H 2.54, N 10.07; Found: C 50.04, H 2.52, N 9.91.

1,2-bis[5-methoxy-2-(3-pyridyl)thiazin-4-yl] perfluorocyclopentene (**1d**)

Yield, 35.1 %. ^{1}H NMR ($CDCl_3$, 300 MHz): δ=8.97–8.96 (m, 2H), 8.63–8.60 (m, 2H), 8.14–8.10 (m, 2H),

7.38–7.33 (m, 2H), 3.89 (s, 6H). ^{13}C NMR ($CDCl_3$, 75 MHz): δ=163.8, 150.5, 150.0, 146.7, 131.0, 129.5, 126.3, 123.8, 115.9, 64.5. Calcd. for $C_{23}H_{14}N_4O_2S_2F_6$: 556.0462, HRMS m/z: 556.0456. Anal. Calcd for $C_{23}H_{14}N_4O_2S_2F_6$: C 49.64, H 2.54, N 10.07; Found: C 49.55, H 2.34, N 9.91.

1-[5-methoxy-2-(3-pyridyl)thiazin-4-yl]-2-[5-methoxy-2-(4-pyridyl)thiazin-4-yl]perfluorocyclopentene (**1e**)

Yield, 30.5 %. ^{1}H NMR ($CDCl_3$, 300 MHz): δ=8.96–8.95 (m, 1H), 8.76–8.61 (m, 3H), 8.11–8.08 (m, 1H), 7.67–7.65 (m, 2H), 7.38–7.30 (m, 1H), 3.89 (s, 3H), 3.88 (s, 3H). ^{13}C NMR ($CDCl_3$, 75 MHz): δ=164.5, 163.9, 150.5, 150.4, 150.0, 149.9, 146.6, 140.1, 132.7, 129.3, 126.5, 126.0, 123.7, 121.0, 119.3, 116.1, 115.8, 115.5, 64.5, 64.4. Calcd. for $C_{23}H_{14}N_4O_2S_2F_6$: 556.0462, HRMS m/z: 556.0466. Anal. Calcd for $C_{23}H_{14}N_4O_2S_2F_6$: C 49.64, H 2.54, N 10.07; Found: C 50.01, H 2.93, N 9.67.

Characterization of the Ring-closed Forms

2a: ^{1}H NMR ($CDCl_3$, 300 MHz): δ=8.74–8.71 (m, 2H), 8.30–8.27 (m, 2H), 7.88–7.83 (m, 2H), 7.50–7.46 (m, 2H), 3.63 (s, 6H). Anal. Calcd for $C_{23}H_{14}N_4O_2S_2F_6$: C 49.64, H 2.54, N 10.07; Found: C 49.60, H 2.57, N 10.18.
2b: ^{1}H NMR ($CDCl_3$, 300 MHz): δ=9.17–9.16 (m, 1H), 8.81–8.80 (m, 1H), 8.74–8.73 (m, 1H), 8.32–8.27 (m, 2H), 7.90–7.87 (m, 1H), 7.51–7.44 (m, 2H), 3.63 (s, 3H), 3.59 (s, 3H). Anal. Calcd for $C_{23}H_{14}N_4O_2S_2F_6$: C 49.64, H 2.54, N 10.07; Found: C 49.41, H 2.97, N 9.58.
2c: ^{1}H NMR ($CDCl_3$, 300 MHz): δ=8.83–8.82 (m, 2H), 8.75–8.73 (m, 1H), 8.31–8.29 (m, 1H), 7.91–7.85 (m, 3H), 7.53–7.49 (m, 1H), 3.64 (s, 3H), 3.61 (s, 3H). Anal. Calcd for $C_{23}H_{14}N_4O_2S_2F_6$: C 49.64, H 2.54, N 10.07; Found: C 49.79, H 2.61, N 10.23.
2d: ^{1}H NMR ($CDCl_3$, 300 MHz): δ=9.17–9.16 (m, 2H), 8.84–8.82 (m, 2H), 8.38–8.36 (m, 2H), 7.55–7.51 (m, 2H), 3.60 (s, 6H). Anal. Calcd for $C_{23}H_{14}N_4O_2S_2F_6$: C 49.64, H 2.54, N 10.07; Found: C 49.67, H 2.86, N 9.78.
2e: ^{1}H NMR ($CDCl_3$, 300 MHz): δ=9.16–9.15 (m, 1H), 8.84–8.82 (m, 3H), 8.34–8.30 (m, 1H), 7.81–7.79 (m, 2H), 7.50–7.45 (m, 1H), 3.60 (s, 6H). Anal. Calcd for $C_{23}H_{14}N_4O_2S_2F_6$: C 49.64, H 2.54, N 10.07; Found: C 49.41, H 2.97, N 9.58.

Results and Discussion

Photochromic Fluorescence Switching

The photo-physical data of the **MPT**-based DAEs **1a–e** were collected in Table 1. Due to the structural similarity, the photochromes **1a–e** showed the similar photochemical properties. To simplify the presented description, we selected **1a** to exemplify the following results and discussions except where otherwise specifically stated.

Table 1 Optical data of all **MPT**-based DAEs in CH_2Cl_2.[a] Maxima of absorption λ_{abs} and of fluorescence emission λ_{em}, molecular absorption coefficients ε_{max}±5 %, and fluorescence quantum yields Φ±5 %[b]

Compound	λ_{abs} (nm)	log(ε_{max}/M^{-1} cm^{-1})	λ_{em} (nm)	Φ
1a	337	4.57	460	<0.01
1b	332	4.54	502	<0.01
1c	336	4.53	514	<0.01
1d	326	4.33	–[c]	
1e	335	4.42		
2a	566	3.93	nonfluorescent	
2b	560	3.93		
2c	563	3.98		
2d	532	3.58		
2e	551	3.86		
P1a	409	4.61	508	0.13
P1b	383	4.40	526	0.11
P1c	398	4.62	540	0.21
P1d	354	4.30	460	0.07
P1e	390	4.44	530	0.13
P2a	596	3.96	nonfluorescent	
P2b	582	3.93		
P2c	599	3.99		
P2d	556	3.53		
P2e	579	3.91		

[a] All spectra were recorded at 293 K

[b] Relative quantum yields were evaluated using quinine sulfate in 0.5 M H_2SO_4 as the standard compound

[c] Difficult to obtain accurate data because of the low fluorescence quantum yields

Upon irradiation with 320 nm lights, the colorless solution of **1a** in CH_2Cl_2 turned purple, showing an absorption maximum at 566 nm (Fig. 1a). The purple color should be due to the closed form **2a**, which showed a high thermal stability (>18 h at 80 °C) but could be bleached by irradiation with visible light. From the ^{1}H NMR spectra of **1a** before and after irradiation with 320 nm light, the resonance of the methoxy proton at 3.85 ppm of **1a** decreased in intensity, while a new singlet of the methoxy proton of **2a** appeared at 3.63 ppm (Fig. S1-5). The ring-closure conversion yield of **1a** was accordingly calculated (Table S1). Therefore, **1a** was characterized as a photochromic molecule.

Fluorescence of **1a–e** should be ascribed to the introduction of the covalently linked **MPT** moieties, in which the fluorescence was originated from the internal charge transfer (ICT) from the methoxy group to the pyridyl group [21]. In the other hand, the existed para-fluoro substituent in the molecular skeleton weakened the ICT process due to its strong electron-

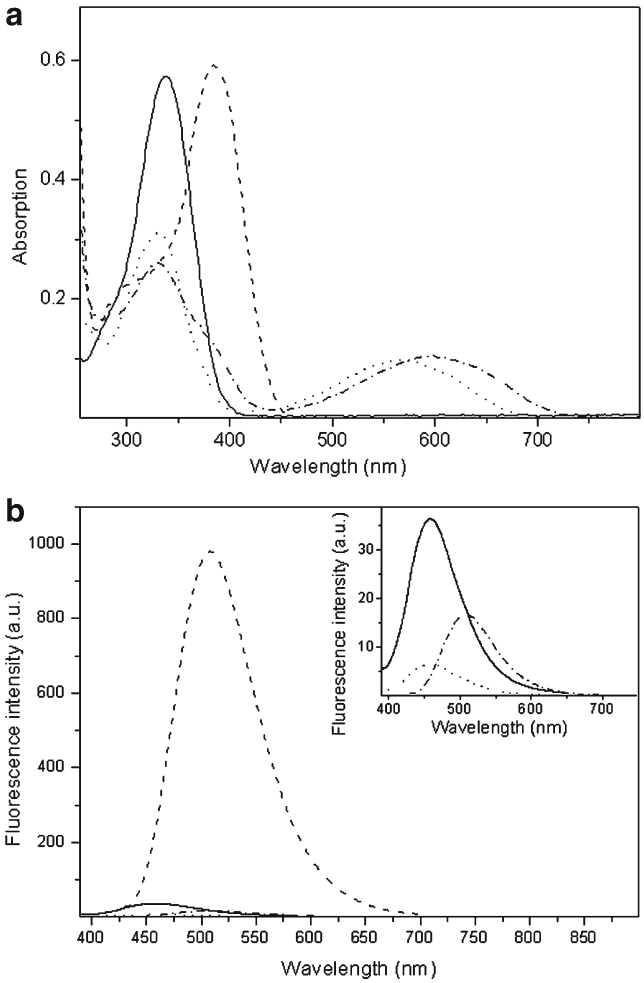

Fig. 1 Absorption (**a**) and fluorescence (**b**) spectra of all four states of the presented system ([**1a**]=2.5×10^{-5} M) in CH_2Cl_2 at 25 °C; *solid line*: the open form **1a**; *dotted line*: PSS; *dashed line*: the protonated open form **P1a**; *dash-dotted line*: the protonated PSS. *Inset*: expansion of the fluorescence from 390 to 650 nm. The emissions of free and protonated forms were excited at 380 and 420 nm, respectively

withdrawing abilities and thus disastrously lowered the quantum yields of fluorescence of **1a**–**e**, even undetectable for compounds **1d**–**e** (Table 1). Photochromes **1a**–**c** were thus investigated as photo-optical switches according to their observable fluorescence.

Irradiated upon UV light, the exhibited fluorescent emission of **1a** at 460 nm gradually decreased down to about 20 % in intensities when arrival at the PSS (Fig. 1b). Considering that photo-cyclization generally changed the orbital hydridization of the reactive carbons attached the methoxy group from sp^2 to sp^3 [10], the coplanarity between the donor and acceptor in **MPT** moieties, which is crucial to the fluorescence, would be destroyed and thus resulted in loss of fluorescence. Thus, the ring-closed forms **2a**–**c** should be non-fluorescent. The observed fluorescence of PSS state should be ascribed to the remained ring-open form **2a** in the system. The photo-cyclization conversion yield calculated from the decrease of emission intensities was in agreement to the values obtained from the ^{1}H NMR experimental (Table S1). In the other hand, the fluorescence could be restored by irradiation with the visible light. Compounds **1a**–**c** were thus proposed as photochromic fluorescent switches.

Protonation Effects on Both Photochromism and Emission

Protonation effects were further investigated for the presented systems. After addition of trifluoroacetic acid (TFA), it could be observed that the absorption maxium of the ring-open form **1a** was remarkably red-shifted from 337 to 409 nm. Irradiation of the protonated form **P1a** by UV light also resulted in the photo-cyclization. The corresponding ring-closed form **P2a** showed a bathochromic shift from 566 to 596 nm in the absorption spectra (Fig. 1a). Emission maximum of **P1a** was also found to be red-shifted to 508 nm accompanied with a significant enhancement of the intensities after addition of 1*M* TFA (Fig. 1b). The effects of protonation on both the absorption and fluorescence should be ascribed to the effects of the protonated pyridyl group on the ICT and transition energy [21].

Accompanied with the protonation-enhanced emission, the photo-cyclization rate of compound **2a** decreased about 14 times compared to the one of free from **1a**. The photo-cyclization rates were evaluated from the time-progressive fluorescences of both the free and protoanted forms, respectively (Fig. 2). For the measurements of the initial velocities, the decreases in the emission intensities at 460 and 508 nm were monitored in the periods of consuming 10 % of the starting free and protonated forms, respectively. Fitted by zero-order reaction kinetics [23], the photo-cyclization rate constants were evaluated as 2.36×10^{-3} s^{-1} and 1.74×10^{-4} s^{-1} for **1a** and **P1a**, respectively (Fig. 2, Table S1). Because the fluorescent emission and photo-cyclization should be the competitive energy relaxation pathways from the excited states, it was obvious that the enhanced quantum yield of fluorescence should be paid by the decrease of photo-cyclization rate. In the other hand, **P2a** was found to be inert to the visible light irradiation for 120 h, which may be caused by the protonation-deprotonation equilibrium of the pyridyl group at the excited states [21]. The controlled photoreactivities, which could be defined as the gated photochromism, was not preferable to non-destructive readout because no ideal output optical could be utilized for the protonated PSS state. Anyhow, the effects of protonation on the absorption, fluorescence, and photochromism of the presented systems could be removed by addition of triethylamine (TEA).

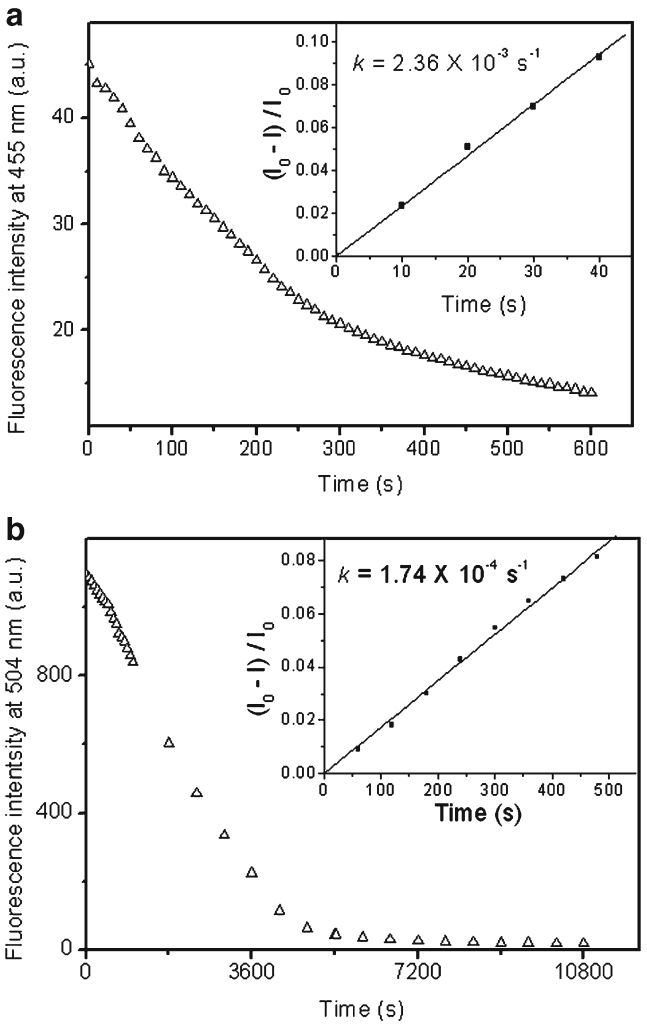

Fig. 2 Time-progressive curves at fluorescent emissions at 460 and 508 nm of **1a** (**a**) and **P1a** (**b**) irradiated at 380 and 420 nm, respectively. The zero-order reaction rates fitting were shown in the corresponding insets, where I_0 and I are the emission intensities at t=0 s and t, respectively

Logic Functions and Molecular Keypad Lock

The transformation among different states could be denoted as the binary Boolean logic functions (Fig. 3). Combined the proton-enhanced and photo-switched fluorescence of **1a**, an INH logic gate was constructed regarding the fluorescence at 508 nm as the output O1 in response to the two external stimuli, protons and UV irradiation, respectively. The fluorescent intensity was high only when the proton was introduced independently. The same input signals also triggered the absorption changes in UV–vis region, which were described by a reconfigurable INH-NOR-YES logic gates utilizing the absorption changes at 389, 337, and 585 nm as the output channels O2, O3, and O4, respectively. Especially, the two outputs, the fluorescence O1 and the absorption at 389 nm O2, produce an INH-INH logic gate keeping synchronous at the two parallel channels. The changes induced by the input signals, proton and UV irradiation, could be compensated by introduction of base and visible light as the corresponding reset operations.

As mentioned above, **P2a** was inert to the irradiation by visible light. Coincidentally, if the **P2a** form was assigned as a "locked" state of a molecular keypad lock while the protonation-enhanced fluorescence of the **P1a** form was denoted as the output signal of the "unlocked" state, the conversion from **P2a** to **P1a** must follow a strict input sequence. Starting with the proton-locked **P2a**, the first input of base (E) produced a neutral form **2a**, and a second input of visible light irradiation (V) converted the ring-closed isomer **2a** to the ring-open isomer **1a**. The "unlocked" state **P1a** could be identified only when a third input of TFA (A) was applied, which produced an intense emission output signal above the threshold. Both input signals and sequence were indispensable for the observation of the intensive emission band at 508 nm (Fig. 1b). In the other word, out of six possible input combinations (EVA, EAV, AEV, AVE, VEA, and VAE), only the EVA input combination could reach the "open" form **P1a** with strong fluorescence signal. Other input strings failed to open the locked state **P2a**. The system capable of authenticating a three digit password entry was thus suggested as a molecular keypad lock (Fig. 4).

a

I_1 Proton	I_2 UV light	O_1 FL at 508 nm	O_2 409 nm	O_3 337 nm	O_4 585 nm
0	0	0 (19.6)	0 (0.056)	1 (0.575)	0 (0.003)
0	1	0 (3.5)	0 (0.031)	0 (0.303)	1 (0.091)
1	0	1 (972.9)	1 (0.584)	0 (0.275)	0 (0.001)
1	1	0 (16.6)	0 (0.112)	0 (0.253)	1 (0.102)

b

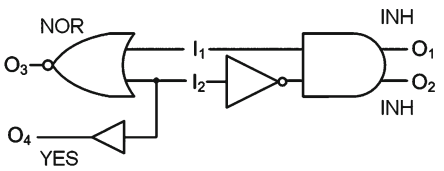

Fig. 3 **a** Truth table of logic gates. **b** INH-INH-NOR-YES logic gates

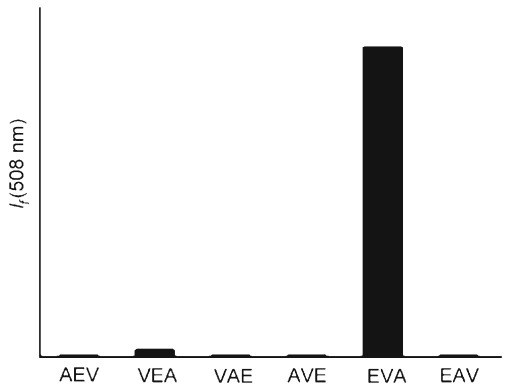

Fig. 4 Molecular keypad lock: output states for different input sequences. The output channel was selected as the fluorescent intensities at 508 nm; the input strings, such as *EVA*, corresponded to the six possible input sequences, where *E*, *V*, and *A* represented TEA, irradiation by visible lights (>550 nm), and TFA, respectively

As shown in most of molecular keypad locks reported, the reset operation were generally involved in the specific input strings as the same strict as the "unlock" operation demanded. Here, the illustrated molecular keypad locks could arrive at the locked state in one-key operation. In the other word, UV irradiation (V) as one lock key could transform the "unlocked" state **P1a** to the "locked" state **P2a** (Scheme 2), which was rarely concerned in previous reports [17, 18]. Such one-key "lock" operation, which acted as the "screen lock" key exemplified in some current intelligent mobiles, could facilitate the applications of the molecular keypad locks in information protection at the molecular levels (Fig. S16).

Conclusions

In conclusion, we synthesized a series of **MPT**-based DAE compounds as photochromic fluorescent switches. Protonation could effect their fluorescent emission as well as photochromic actions, i.e., enhanced fluorescence and gated photochromism, respectively. Because the protonation and photo-isomerization reactions provide reversible changes in absorption and fluorescence spectra, we then constructed parallel INH-INH-NOR-YES logic gates. Further, assigned the protonated ring-open forms and the protonated ring-closure forms as unlocked and locked states, respectively, molecular keypad locks were thus accomplished. Notably, from the unlocked state, one-key lock operation could be achieved by the direct UV irradiation.

References

1. Irie M (2000) Diarylethenes for memories and switches. Chem Rev 100:1685–1716
2. Gust D, Andréasson J, Pischel U, Moore TA, Moore AL (2012) Data and signal processing using photochromic molecules. Chem Commun 48:1947–1957
3. Cusido J, Deniz E, Raymo FM (2009) Fluorescent switches based on photochromic compounds. Eur J Org Chem 2009:2031–2045
4. Yun C, You J, Kim J, Huh J, Kim E (2009) Photochromic fluorescence switching from diarylethenes and its applications. J Photochem Photobiol C 10:111–129
5. Yildiz I, Deniz E, Raymo FM (2009) Fluorescence modulation with photochromic switches in nanostructured constructs. Chem Soc Rev 38:1859–1867
6. Tian H, Feng Y (2008) Next step of photochromic switches? J Mater Chem 18:1617–1622
7. Tian H, Wang S (2007) Photochromic bisthienylethene as multifunction switches. Chem Commun 43:781–792
8. Irie M, Fukaminato T, Sadaki T, Tamai N, Kawai T (2002) A digital fluorescent molecular photoswitch. Nature 420:759–760
9. Kawai SH, Gilat SL, Lehn J-M (1999) Photochemical pKa-modulation and gated photochromic properties of a novel diarylethenes switch. Eur J Org Chem 1999:2359–2366
10. Yumoto K, Irie M, Matusda K (2008) Control of the photoreactivity of diarylethene derivatives by quaternarization of the pyridylethynyl group. Org Lett 10:2051–2054
11. Poon C-T, Lam WH, Yam VW-W (2011) Gated photochromism in triarylborane-containing dithienylethenes: a new approach to a "lock-unlock" system. J Am Chem Soc 133:19622–19625
12. Kutsunugi Y, Coudret C, Micheau JC, Kawai T (2012) Photomodulation of the proton affinity and acid gated photochromism of a novel dimethylaminophenyl thiazoles diarylethenes. Dye Pigment 92:838–846
13. Zhu W, Song L, Yang Y, Tian H (2012) Novel bisthienylethene containing ferrocenyl-substituted naphthalimide: a photo- and redox multi-addressable molecular switch. Chem Eur J 18:13388–13394
14. Wu Y, Chen S, Yang Y, Zhang Q, Xie Y, Tian H, Zhu W (2012) A novel gated photochromic reactivity controlled by complexation/dissociation with BF_3. Chem Commun 48:528–530
15. Margelies D, Felder CE, Melman G, Shanzer A (2007) A molecular keypad lock: a photochemical device capable of authorizing password entries. J Am Chem Soc 129:347–354
16. Rout B, Milko P, Iron MA, Motiei L, Margulies D (2013) Authorizing multiple chemical passwords by a combinatorial molecular keypad lock. J Am Chem Soc 135:15330–15333
17. Andréasson J, Straight SD, Moore TA, Moore AL, Gust D (2009) An all-photonic molecular keypad lock. Chem Eur J 15:3936–3939
18. Andréasson J, Pischel U, Straight SD, Moore TA, Moore AL, Gust D (2011) All-photonic multifunctional molecular logic device. J Am Chem Soc 133:11641–11648
19. Zou Q, Li X, Zhang J, Zhou J, Sun B, Tian H (2012) Unsymmetrical diarylethenes as molecular keypad locks with tunable photochromism and fluorescence via Cu^{2+} and CN^- coordinations. Chem Commun 48:2095–2097
20. Chen S, Guo Z, Zhu S, Shi W, Zhu W (2013) A multiaddressable photochromic bisthienylethene with sequence-dependent responses: construction of an INHIBIT logic gate and a keypad lock. ACS Appl Mater Interfaces 5:5623–5629
21. Zheng M-H, Jin J-Y, Sun W, Yan C-H (2006) A new series of fluorescent 5-methoxy-2-pyridylthiazoles with a pH-sensitive dual-emission. New J Chem 30:1192–1196
22. Li Z-X, Sun W, Yue Y-F, Zheng M-H, Xu C-H, Jin J-Y, Fang C-J, Yan C-H (2007) Synthesis of a solvent-sensitive highly fluorescent derivative of perfluorocyclopentene. Tetrahedron Lett 48:7675–7679
23. de Jong JJD, Lucas LN, Hania R, Pugzlys A, Kellogg RM, Feringa BL, Duppen K, van Esch JH (2003) Photochromic proterties of perhydro- and perfluorodithienylcyclopentene molecular switches. Eur J Org Chem 2003:1887–1893